POLITECNICO DI TORINO
Repository ISTITUZIONALE

A new approach in the implementation of insulating layers in soft magnetic composite materials

Original
A new approach in the implementation of insulating layers in soft magnetic composite materials / Poškovi, E., Franchini, F., Grande, M.A., Ferraris, L., Carosio, F., Tenconi, A.. - In: JOURNAL OF MAGNETISM AND MAGNETIC MATERIALS. - ISSN 0304-8853. - ELETTRONICO. - 597:(2024). [10.1016/j.jmmm.2024.171984]

Availability:
This version is available at: 11583/2989264 since: 2024-06-03T16:39:25Z

Publisher:
Elsevier

Published
DOI:10.1016/j.jmmm.2024.171984

Terms of use:

This article is made available under terms and conditions as specified in the corresponding bibliographic description in the repository

Publisher copyright

(Article begins on next page)

15 November 2026

Journal of Magnetism and Magnetic Materials 597 (2024) 171984



Contents lists available at ScienceDirect

Journal of Magnetism and Magnetic Materials

journal homepage: www.elsevier.com/locate/jmmm





A new approach in the implementation of insulating layers in soft magnetic composite materials

Emir Pošković [a,*], Fausto Franchini [a], Marco Actis Grande [b], Luca Ferraris [a], Federico Carosio [b], Alberto Tenconi [a]

[a] Energy Department, Politecnico di Torino, Torino, Italy
[b] Department of Applied Science and Technology, Politecnico di Torino, Torino, Italy

ARTICLE INFO

Keywords:
Soft Magnetic Composite (SMC)
Layer-by-Layer technique
Organic and Inorganic Layer
Iron losses
Polyethilenimine
Clay
Silicates, Silica

ABSTRACT

Soft Magnetic Composite (SMC) materials show a high potential for growth in the electrification of several industrial sectors for two main reasons: the reduced eddy current losses and the 3D magnetic path which allows to redesign magnetic circuits without geometrical constraints. On the other hand, some material limitations and process restrictions limit the use of SMC on a large scale; this contribution aims to overcome such constraints through a novel surface approach using a Layer-by-Layer (LbL) technique that allows to coat each particle with a nanostructured layer, providing electrical insulation enhanced mechanical strength and withstanding higher treatment temperatures. Four SMCs encompassing the developed innovative multi-functional layers have been prepared and deeply analyzed with a characterization campaign through the study of the surface morphology with a Scanning Electron Microscope (SEM), the magnetic properties with a Single Sheet Tester (SST) and the mechanical strength through the "Transverse Rupture Strength" (or TRS) test. The discussion on the results has to be considered a starting point for future investigations, as each of the four different systems represents a partial solution to a specific SMC problem. Also, some considerations on the possible application are proposed.

1. Introduction

Electrification in various industrial sectors is a primary goal and depends on developing functional materials such as magnets [1]. Magnetic materials are subdivided in soft and hard. The hard materials are permanent magnets; it is important to remember that the Rare Earth alloys, sintered or bonded, are crucial for electrical transporting [2]. Their actual economic status affects various industrial applications, and some studies are promoted to find alternative solutions or recycling [3–6]. Instead, soft magnetic materials are a larger world compared to permanent magnets. Various families of soft magnetic materials are used and strictly connected to applications [7]. For example, specific magnetic materials are commonly used for electrical machines, industrial power and signal electronics, telecommunications, informatics, etc [8]. Considering these aspects, our studio will focus only on soft magnetic materials used to improve efficiency and design for electrical machines and static conversion. A magnetic material that shows different potentials, such as high geometric flexibility, reduced iron losses in several frequency ranges, and a 3D magnetic path, is Soft Magnetic Composite (SMC) [9].

Such materials are employed in a growing number of applications [10]. The SMC materials are part of the soft magnetic circuit of electrical machines and inductances. The electrical machines require far saturation, high maximum permeability and low iron losses below 2 kHz [11]. The inductances benefit from high initial permeability, imaginary permeability near zero, and very low losses until the MHz range [12]. Electrical machines generally use laminated sheets, but new proposed efficient motor designs show different geometrical limitations. Soft ferrites are widely used in electronic devices; conversely, they are very brittle [13]. Additive manufacturing materials show high potential for new geometrical design, but actual high eddy current losses and complex process setup limited their diffusion and required further optimization [14–18]. The different behaviours mentioned above can be obtained through the selection of the core powder size and, more importantly, through the layer's nature and properties.

The SMCs show low eddy current losses for different frequencies and can be produced in very complex geometries [19]. On the other hand, the main disadvantages are the mechanical strength and high-

* Corresponding author.
E-mail address: emir.poskovic@polito.it (E. Pošković).

https://doi.org/10.1016/j.jmmm.2024.171984
Received 4 December 2023; Received in revised form 14 March 2024; Accepted 20 March 2024
Available online 27 March 2024
0304-8853/© 2024 The Author(s). Published by Elsevier B.V. This is an open access article under the CC BY license (http://creativecommons.org/licenses/by/4.0/).

temperature treatment restrictions. The maximum temperature of heat treatment of the commercial products does not exceed 650 °C; also, for this reason, the hysteresis losses remain higher compared to laminated steel. Other motivations for high hysteresis losses are related to the type and dimensions of coating used to cover ferromagnetic particles. The coating formation can be of organic or inorganic origin. Organic materials are based on different polymer materials, especially epoxy and phenolic resins [9,10,20,21]. Examples of inorganic coatings are metal oxides (ferrites, silica, alumina, etc), silicon, and phosphate [9,10,21].

The production of the coating layer consists of a wide variety of techniques. The most famous is based on the use of orthophosphoric acid H_3PO_4 to obtain the layer through the wet chemistry method [22–25]. Also, some particular techniques based on chemical and mechanical processes have been suggested for the silica coating layer [26–30]. The ferrites layer is widely studied as a solution to cover ferromagnetic particles. A variety of techniques are proposed: surface oxidation [31–33], ball milling and spark plasma sintering [34–36], and impact milling [37]. Resins are often used as mechanical binders in inorganic and organic coating systems. The cited state-of-the-art layer compositions pose some limitations due to one or more of the following reasons: insulation lack, poor thermal stability, low thickness uniformity, and low adhesion strength.

To overcome a part of the mentioned limitation, a new method is outlined, based on the Layer-by-layer technique (LbL), in which many different multifunctional layers can be implemented on top of each single core particle. This method involves the immersion of the particles in separate baths, each of them containing a particular substance, reacting by means of electrostatic charge or similar interactions. The method is patented [38,39].

With the proposed technique, many different functional materials were produced, two of them particularly suited for electrical machines and two for mid-low frequency inductances. Various parameters were measured to assess the performance of the proposed SMC materials.

2. Materials and methods

The ferromagnetic powder FeABC 100.30 of company Höganäs is covered by four different layer systems. This powder has very low oxygen content (0.04 wt%) and is usually used as baseline powder for the SMCs. The average particle size of the proposed powder is about 100 μm. The preparation of new insulating coatings for ferromagnetic powder starts with the use of the layer-by-layer deposition (LbL) technique [40–42]. The not complex procedure allows to obtain a very thin layer of nanometer dimensions and a heterogeneous multifunctional insulating magnetic composite material. The coating compositions included various components of organic and/or inorganic origins. The correct choices of components permit the production of positively or negatively charged solutions/suspensions baths to be employed for the LbL deposition. Typically, the baseline ferromagnetic powder is alternatively exposed to both positive and negative baths, allowing the components to be adsorbed. This kind of deposition prepares a nanostructured coating comprising multiple layers held together by electrostatic interactions. The deposition step is followed by the particles washing in the deionized water. The detachment of the ferromagnetic powder from the deposition/washing bath is obtained using centrifugal forces or magnetic separation. The process can be repeated until the designed number of deposited layers is reached, as illustrated in Fig. 1. At the end of the procedure, the covered powders were dried in a vacuum oven at 80 °C.

As previously mentioned, four different composition systems have been prepared, where each half layer is obtained in a stable deionized watery solution/suspension of 75 ml of predetermined charge [43]. Deionized water, with a high purity of 18.2 MΩ·cm, is obtained through a Q20 Millipore system (Italy). The iron powder shows a negative charge in the water related to chemical aspects. The reagents used in watery solution/suspension are Polyethilenimine branched BPEI polymer in gel form [40,43], Polyacrylic acid PAA diluted in 35 wt% in water [43,44], Montmorillonite *K*10 in powder form [45], Sodium Silicate [46], LUDOX® TM-40 colloidal silica 40 wt% suspension in water, and Magnetite-Iron (II, III) oxide nanopowder (50–100 nm particle size) were purchased from Merck in Darmstadt, Germany. Boehmite DISPERAL is supplied by SASOL in Brunsbüttel, Germany [47].

- **System#1**, based on 1.5 layers deposited in the following steps: Polyethilenimine branched (BPEI) polymer dissolved in water with 0.5 wt% concentration – Montmorillonite (MMT) clay is added in Polyacrylic acid (PAA) and both dissolved in water with 1 wt% and 0.5 wt% concentrations respectively – last half layer with Poliethilenimine branched (BPEI) is the same as the first one. The PAA/MMT solution is adjusted with sodium hydroxide NaOH to obtain a pH of about 8 to avoid powder oxidation. BPEI is based on positively charged amines; therefore, an attractive electrostatic force will be probable. In contrast, the PAA/MMT is negatively charged. The developed coated powder has an organic–inorganic combination coating composition. This powder should be used for magnetic materials where the reduction of eddy current losses is required.
- **System#2**, based on 4 layers deposited in the following steps: Boehmite (AlOOH), transition alumina compounds, dissolved in water with 1 wt% concentration – Sodium Silicates, dissolved in water with 1 wt% concentration. The steps are repeated three times. Boehmite AlOOH is positively charged; on the other hand, the

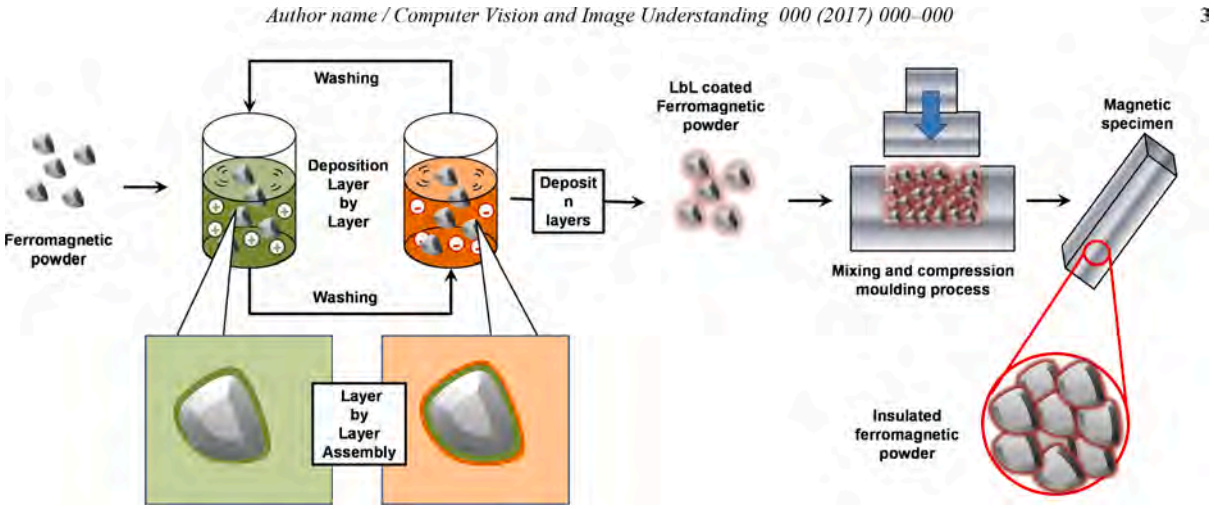


Fig. 1. Multilayered nanostructured insulating coating using Layer by Layer deposition technique.

sodium silicate is negatively charged. The obtained coated powder has a coating with full inorganic behaviour. This powder is studied to obtain better mechanical strength.

- **System#3**, based on a single complex layer deposited in the following steps: the Boehmite ($AlOOH)_2$ dissolved in water with 1 wt % concentration – Colloidal Silica (SiO_2), dissolved in water with 1 wt% concentration, are complexed together in a unique deposition (monolayer). Again, the covered powder has a coating with total inorganic behaviour. The proposed powder should show a high temperature withstanding.
- **System#4**, based on a complex monolayer deposited in the following steps: Polyethilenimine branched (BPEI) filled with Magnetite at 1 wt% and dissolved in water with 0.5 wt% concentration – Montmorillonite (MMT) clay dissolved in water with 1 wt% concentration, are complexed together in a unique layer. The proposed powder is a hybrid coating composition, organic–inorganic, and can be used for high-frequency applications.

All proposed powder systems are compacted in parallelepiped shape (3x10x55 mm) at 800 MPa employing a 200-ton hydraulic press. Therefore, obtained parallelepiped specimens are thermal treated in the oven at different temperatures: system#1 at 180 °C in the air for 60 min, system#2 at 500 °C in the air for 5 min, system#3 at 750 °C in the vacuum for 30 min and system#4 at 300 °C in the air for 16 min. Table 1 reports all the information concerning layer compositions and heat treatments.

2.1. Analysis methodologies

2.1.1. Qualitative analyses

Scanning electron microscope (SEM) of brand Zeiss Evo 15 equipped with Oxford Ultim Max 40 probe is used to investigate in qualitative analyses the achievement of coating of the proposed powders compared to no coated baseline iron. The single sheet tester (SST), which is self-built and self-programmed for magnetic characterisation, is used. It is a soft materials hysteresisgraph where the LabVIEW Virtual Instrument (2012 edition) controls and acquires the required data and parameters. Fluke PM6306, a programmable automatic RCL meter, measures the inductance values. ZwickRoell GmbH &Co. Typ SMT1-FR100TL.A80 is performed for the transverse rupture strength or TRS test. The results of these experiments are reported in the dedicated chapter.

2.1.2. Magnetic analysis with single sheet tester

The magnetic characterization of the laminated steel and SMC materials is performed thoroughly using the Epstein frame and toroidal magnetic test [48]. On the other hand, the single sheet tester (SST) method can also help assess the magnetic characteristics of laminated steel and SMC materials [49–52]. The parallelepiped samples do not need to be wound; in this way, the measurements are immediately performed, saving and adjusting the time of the specimen preparation process. The single sheet tester is equipped with a secondary winding around the sample's middle and a split primary winding at both sides, as illustrated in Fig. 2 [49]. The SST method is a faster application than the mentioned magnetic tests; on the other hand, the calibration with standard tests is performed to adjust the errors in the frequency range.

Table 1
Proposed coating powder systems: compositions, number of layers, heat treatment, and field of application.

Proposed Coating Systems	Number of layers	Compositions	Heat treatment	Possible Applications
System#1	1.5	BPEI-PAA \MMT-BPEI	60 min @180 °C air	Electrical machines to improve the efficiencies
System#2	4	AlOOH-Silicates x 4 times	5 min @500 °C air	Improve mechanical strength
System#3	1 complexed	AlOOH-SiO_2 complexed	30 min @750 °C vacuum	Improve the temperature withstanding
System#4	1 complexed	BPEI\MAG-MMT complexed	15 min @300 °C air	Inductors for medium–high frequencies

2.1.3. Mechanical characterization

The mechanical strength of produced SMC materials can be expressed through the so-called "Transverse Rupture Strength" (or TRS) with a three-point bending test, as shown in Fig. 3. The parallelepiped specimen lends itself to performing the TRS test after magnetic characterization; therefore, the same samples are used. Commonly, the mechanical properties of most SMC materials are relatively low when compared with bulk or laminated metallic materials. The commercial products do not exceed 120 MPa. From these points of view, improving the mechanical properties is a primary challenge for SMC materials.

3. Experimental results

3.1. Microstructure analysis

3.1.1. Iron baseline powder

The first microstructure analysis consists of the investigation of the surface and composition of no-coated iron powder. The powder shows an irregular shape typical of water-atomized iron powder, as shown in Fig. 4. The Energy-Dispersive X-ray Spectroscopy (EDS) composition spectrum shows only iron element peaks, as reported in Fig. 5. It confirms the purity of the iron powder.

3.1.2. Coated powder system#1

It is possible to note, starting from Fig. 6a, the different conformation with respect to baseline iron powder. Fig. 6b shows the formation of high-dense zones similar to the peel, which is more or less regular. Moreover, in Fig. 7, the iron attendance is lower than that of no-coated iron powder, and the elements that characterize the organic layer behaviour are detected. The cover process can be considered distinguished.

3.1.3. Coated powder system#2

The coating seems fluffy, like snow, as shown in Fig. 8b. The presence of iron is around 93 ÷ 94 %, and the typical elements related to silicates and boehmite are reported in Fig. 9. The coated process is not so distinguished as the previous one; on the other hand, the EDS composition confirms the deposition of the layers.

3.1.4. Coated powder system#3

The coated powder is immediately distinguished from other proposed and baseline powders, as shown in Fig. 10. The presence of white colour flakes of different dimensions confirms the good deposition of the complexed monolayer. Further, in Fig. 11, the presence of elements related to boehmite and silica and the high iron content reduction allows to consider a successful coating process.

3.1.5. Coated powder system#4

The coated powder is simply recognized because of pores on the coating layer, as noted in Fig. 12b. Also, the EDS analysis confirms the hybrid organic and inorganic behaviour of the complexed layer, as shown in Fig. 13. The coating process can be considered achieved. In the end, the metallographic analysis is performed without considering the effect of the heat treatments; therefore, some coating layers could have unexpected behaviour.

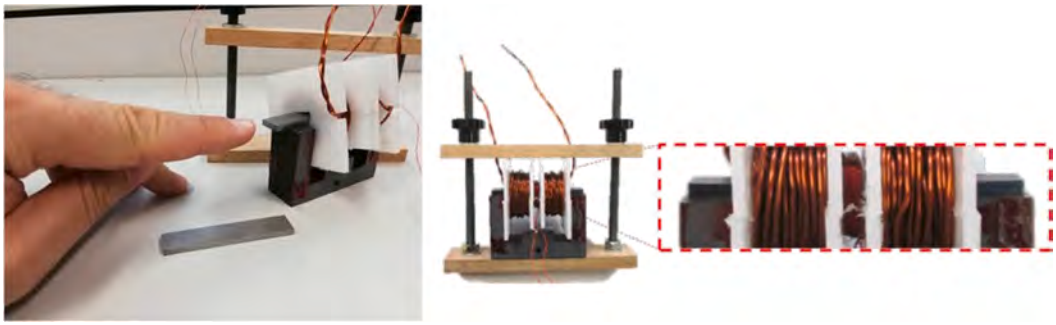


Fig. 2. Single sheet tester setup used for the magnetic characterization.



Fig. 3. Mechanical bending test used for proposed SMC materials.

3.2. Magnetic properties analysis

The magnetic measurements performed by means of the described Single Sheet Tester (Fig. 2) allow to obtain a classification of the proposed systems under the magnetic point of view. They have then been tested to verify the respective magnetic characteristics B(H), the magnetic permeability, the specific losses and the hysteresis cycles related to the frequency of the exciting magnetic field.

3.2.1. Magnetic characterization for coated powder system #1

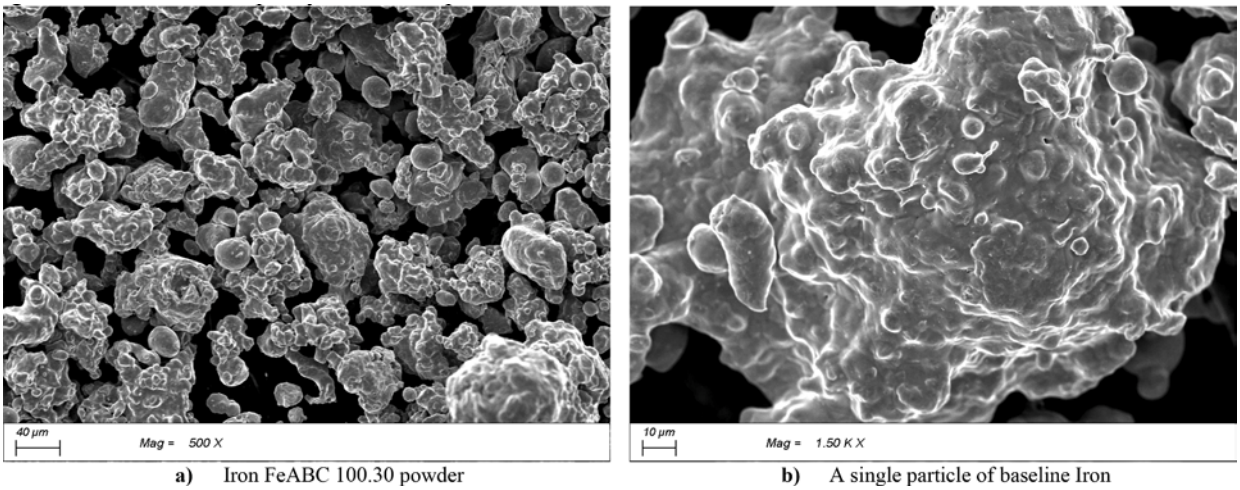
The BH curves and magnetic permeability for different frequency values are reported in Fig. 14. The BH curves show good stability, varying the frequency, and the magnetic induction @5000 A/m is about 1.40 T. The maximum magnetic permeability is 522. The specific iron losses are reported in Fig. 15. For instance, the value @50 Hz and 1 T is 6.52 W/kg. However, the hysteresis cycles at 1 T are illustrated in Fig. 16 for a detailed understanding of the losses behaviour. The cycles are very close, and this means that the proposed material, system#1, shows low eddy current losses due to good electrical insulation between the particles. These results can be considered acceptable for an application in electrical machines.

3.2.2. Magnetic characterization for coated powder system #2

For proposed system#2, the BH curves and magnetic permeability for different frequency values are reported in Fig. 17. The BH curves are less stable with frequency compared to system#1, and these results already imply the presence of substantial eddy current losses. The magnetic induction @5000 A/m is about 1.51 T for several frequencies. The magnetic permeability is also affected by eddy current losses, even though the maximum value is 539. The specific iron losses are reported in Fig. 18, and the value @50 Hz and 1 T is 7.57 W/kg. The hysteresis cycles show the high contribution of dynamic losses, mainly at 1 kHz, as reported in Fig. 19. From the magnetic and energetic point of view, the proposed layer composition could be used in small electrical machines.

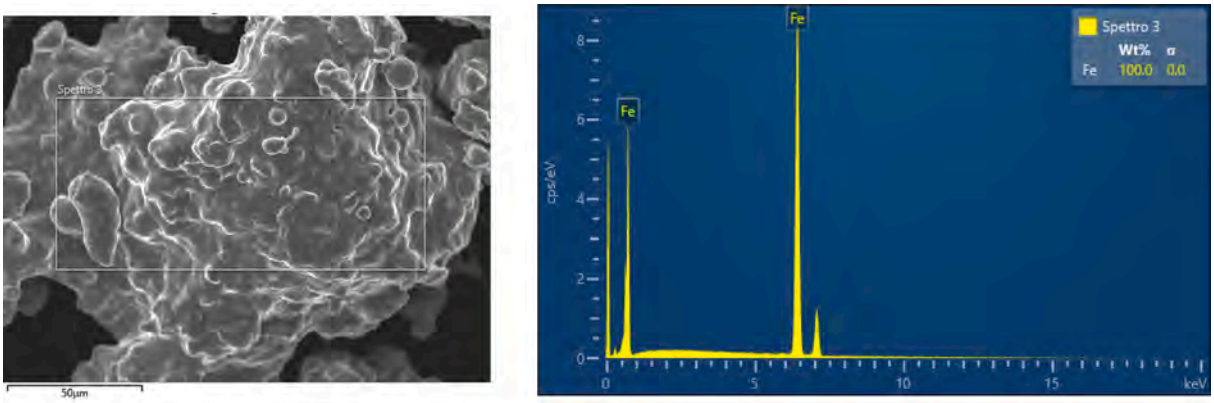
3.2.3. Magnetic characterization for coated powder system #3

System #3 was developed in order to operate at high temperatures, and after the heat treatment at 750 °C, the BH curves and magnetic permeability for different frequency values are shown in Fig. 20. The maximum magnetic permeability is about 200, and magnetic induction @5000 A/m is about 0.85 T for some frequencies. The high eddy currents affect this SMC material, as noted in Fig. 21. Accordingly, the



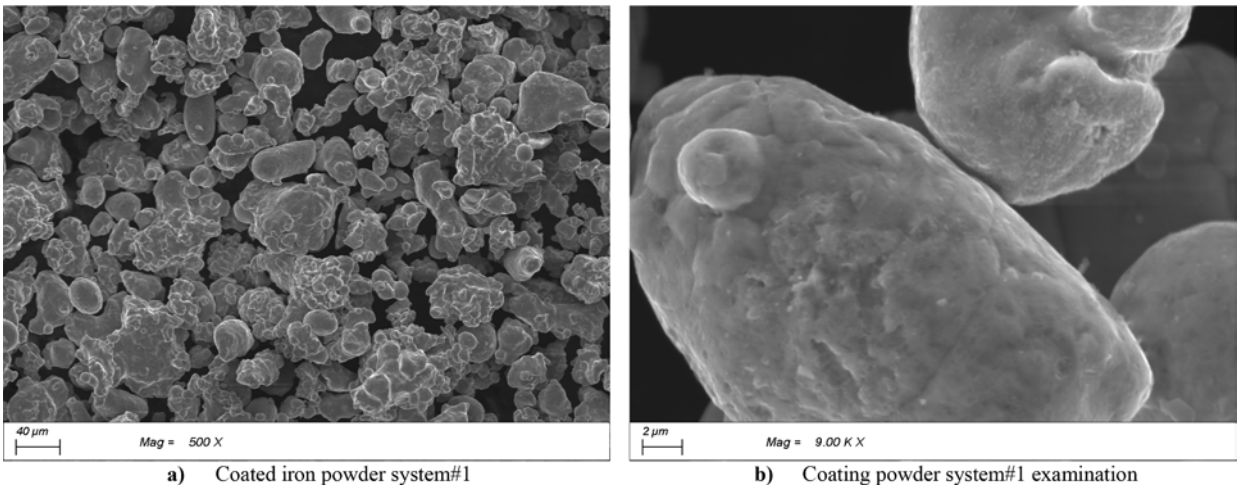
a) Iron FeABC 100.30 powder **b)** A single particle of baseline Iron

Fig. 4. Microstructural analysis by means of SEM for Iron FeABC 100.30 baseline powder.



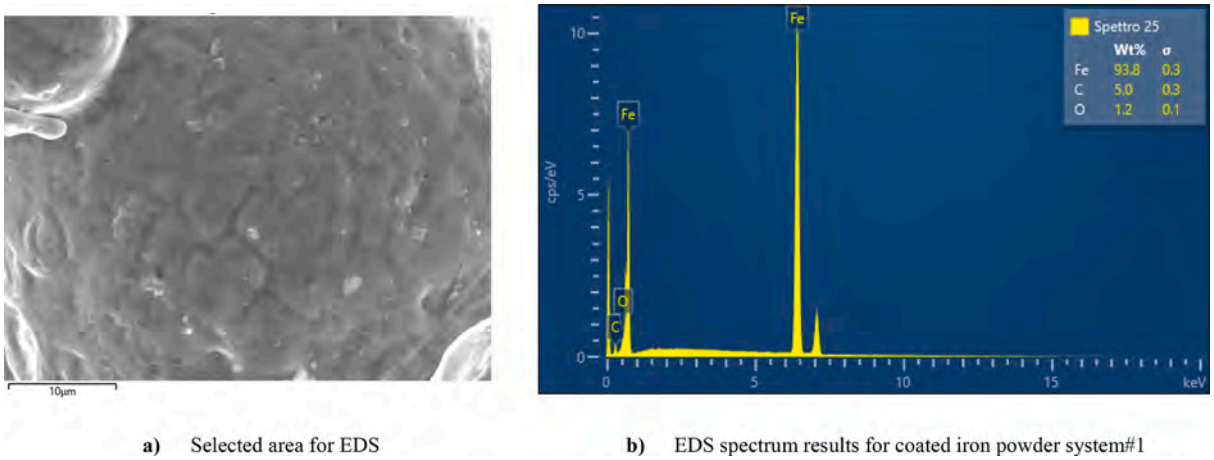
a) Selected area for EDS b) EDS spectrum results for Iron FeABC 100.30 baseline powder

Fig. 5. EDS composition analysis for Iron FeABC 100.30 baseline powder.



a) Coated iron powder system#1 b) Coating powder system#1 examination

Fig. 6. Microstructural analysis by means of SEM for coated iron powder system#1.



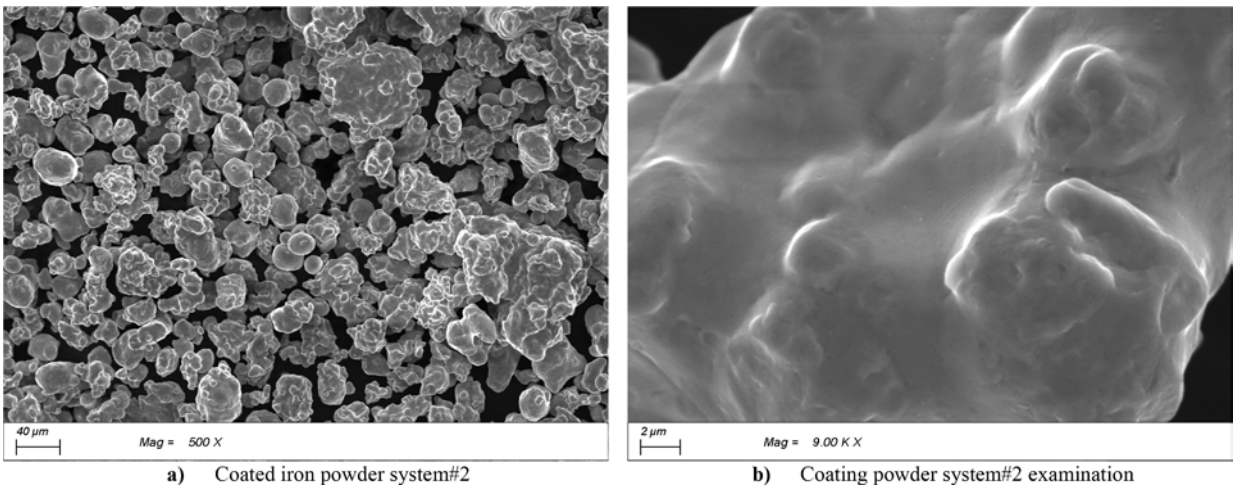
a) Selected area for EDS b) EDS spectrum results for coated iron powder system#1

Fig. 7. EDS composition analysis for coated iron powder system#1.

hysteresis cycles are wider and bent, but surprisingly, they maintain a sigmoidal behaviour at 1 T until 100 Hz, as shown in Fig. 22. For instance, specific iron losses @50 Hz and 1 T is 13.87 W/kg. The proposed SMC material has very high iron losses, but it can be considered a good starting point for studying and optimising a high-temperature layer.

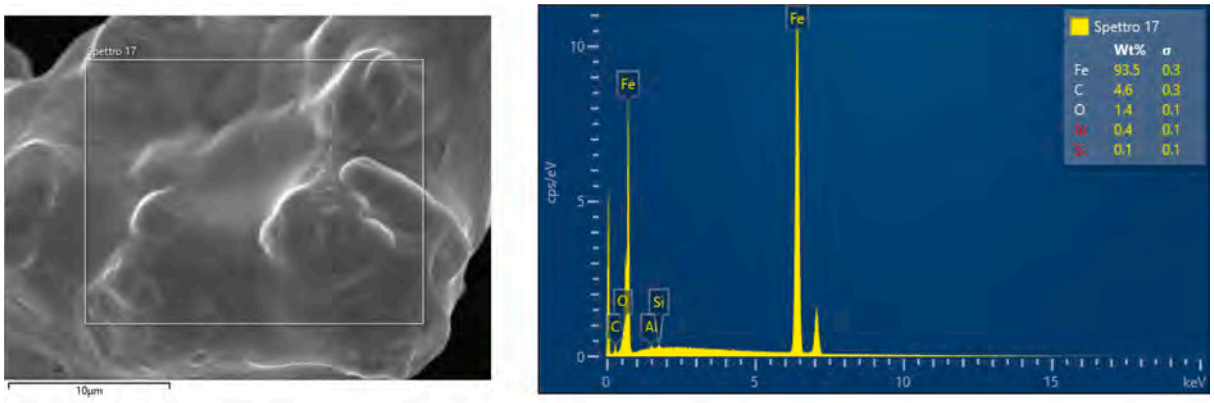
3.2.4. Magnetic characterization for coated powder system #4

The proposed SMC material with coating system#4 shows low eddy current losses. This is understandable, as observed in the stability of the BH curves and magnetic permeability of Fig. 23. The maximum magnetic permeability is 218, and magnetic induction @5000 A/m is 0.84 T. The specific iron losses are reported in Fig. 24, and the value @50 Hz



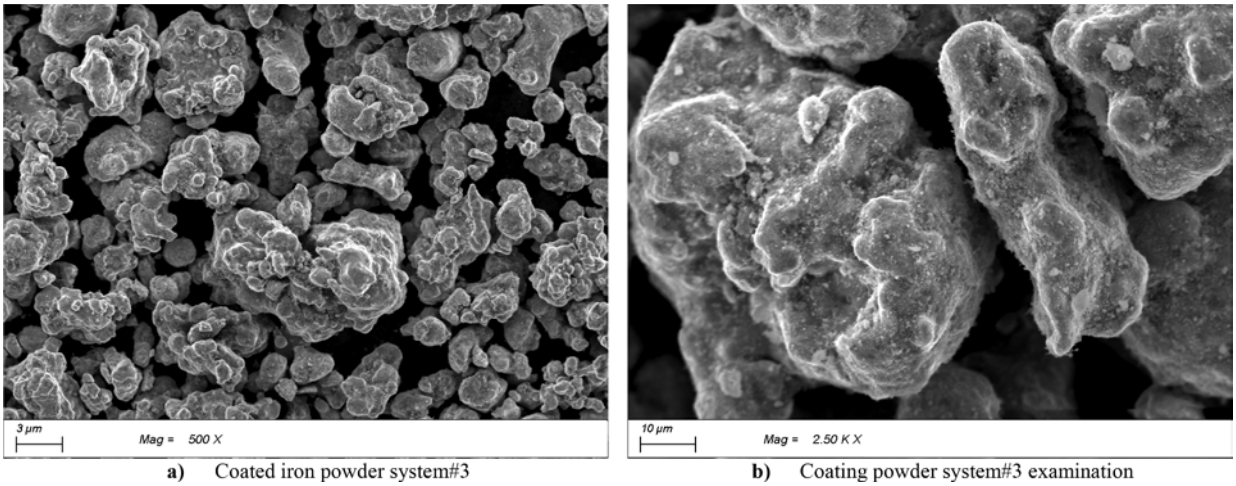
a) Coated iron powder system#2 b) Coating powder system#2 examination

Fig. 8. Microstructural analysis by means of SEM for coated iron powder system#2.



a) Selected area for EDS b) EDS spectrum results for coated iron powder system#2

Fig. 9. EDS composition analysis for coated iron powder system#2.



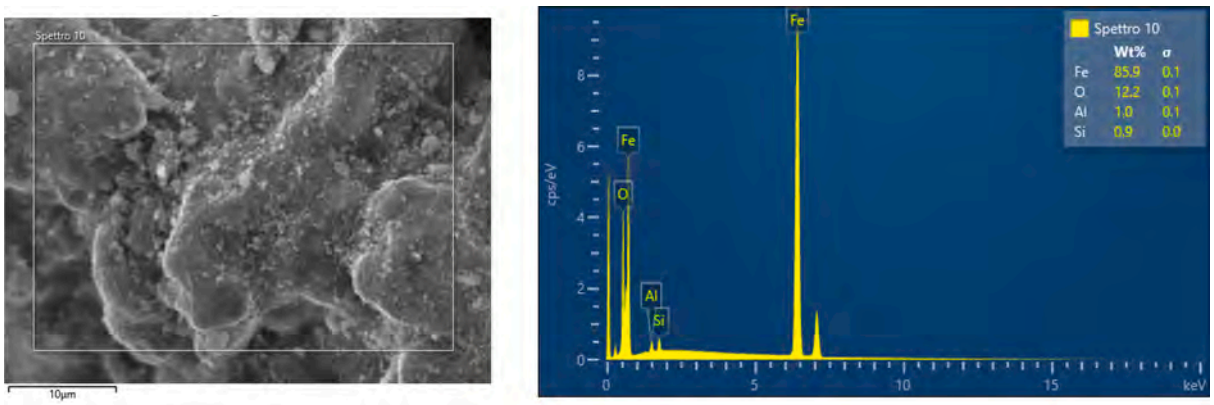
a) Coated iron powder system#3 b) Coating powder system#3 examination

Fig. 10. Microstructural analysis by means of SEM for coated iron powder system#3.

and 1 T is 11.48 W/kg. Also, the hysteresis cycles imply the reduction of eddy current losses in Fig. 25. The filled magnetite in BPEI has increased the bulk electrical resistivity; on the other hand, it did not improve magnetic performance, and the monolayer contributed to increment hysteresis losses. The produced SMC material could be suitable for medium-frequency inductors.

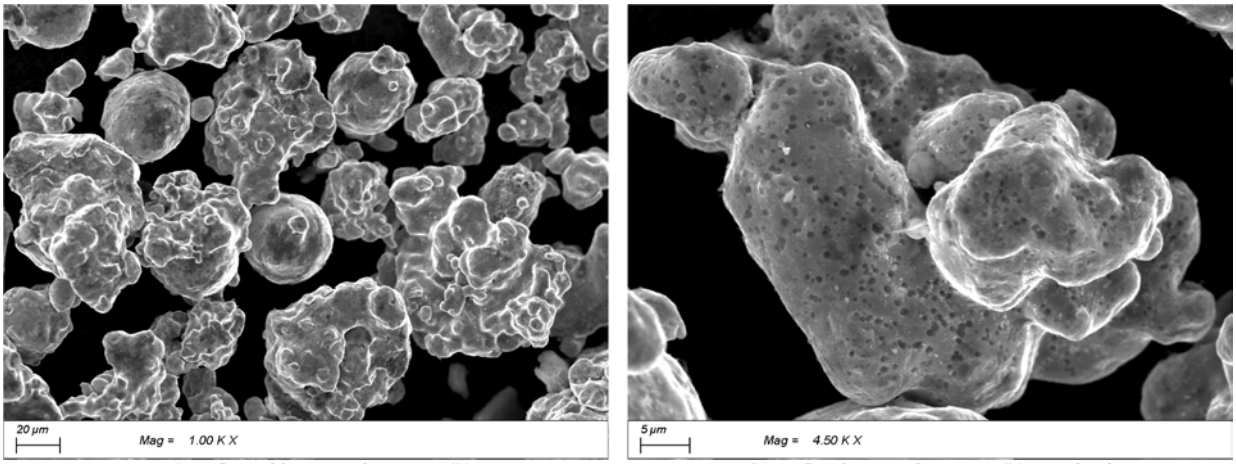
3.3. Mechanical characterization

The mechanical strength of the proposed systems has been verified



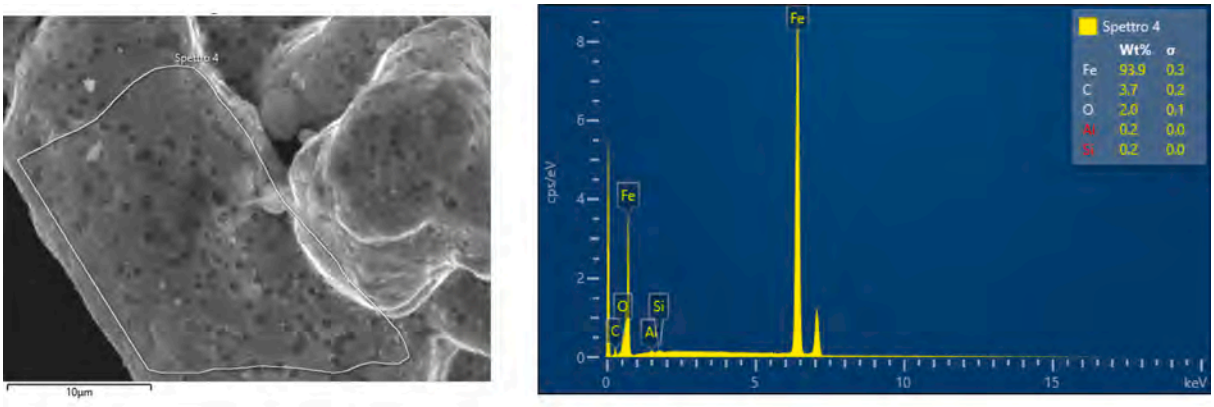
a) Selected area for EDS **b)** EDS spectrum results for coated iron powder system#3

Fig. 11. EDS composition analysis for coated iron powder system#3.



a) Coated iron powder system#4 **b)** Coating powder system#4 examination

Fig. 12. Microstructural analysis by means of SEM for coated iron powder system#4.



a) Selected area for EDS **b)** EDS spectrum results for coated iron powder system#4

Fig. 13. EDS composition analysis for coated iron powder system#4.

with the methodology described in Section 2, and by means of the equipment shown in Fig. 3.

The average mechanical strength results are reported in Table 2. TRS of 110 MPa of system #1 is comparable to other industry-standard SMC materials, of which the present material is a good candidate for an in-place substitution. The SMC with coating system #2 shows promising mechanical strength with a TRS of 191 MPa. In the case of system #3, the TRS is adequate, even if it is expected to be higher due to high-temperature treatment. System #4 has low mechanical properties, but it is suitable for inductance applications.

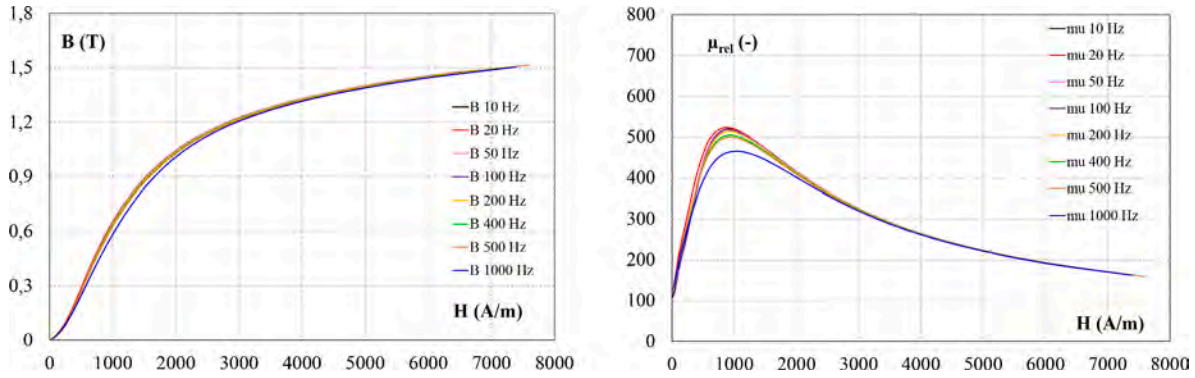


Fig. 14. BH curves and magnetic permeability as a function of the frequency for the system #1.

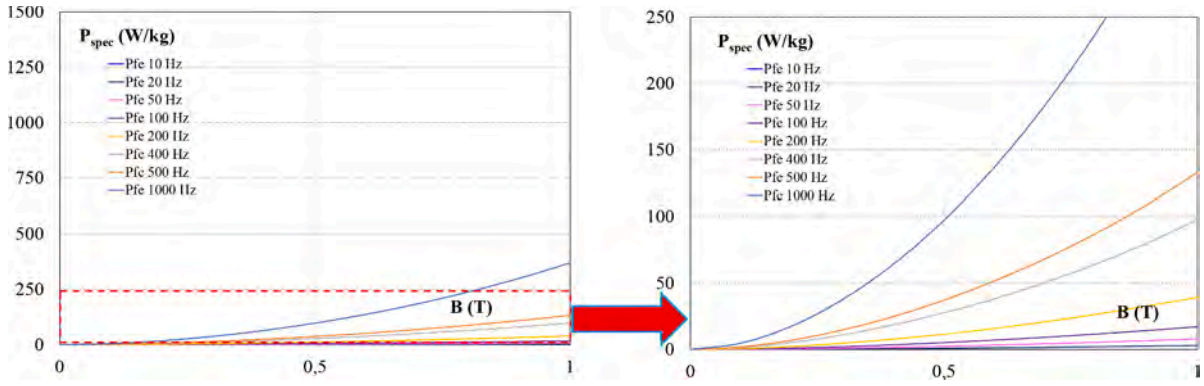


Fig. 15. Specific iron losses as a function of magnetic induction at different frequencies for system #1: full range and restricted to 250 W/kg.

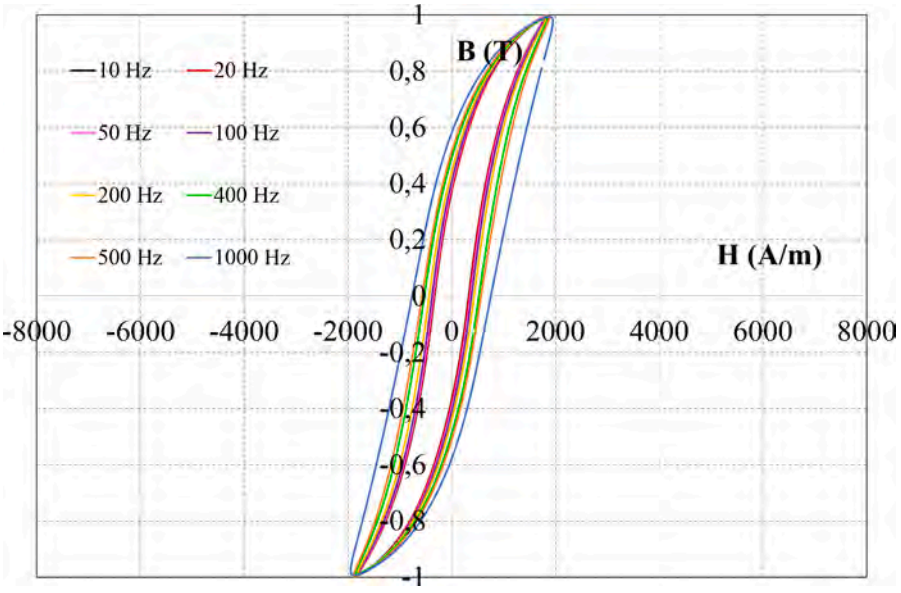


Fig. 16. Hysteresis cycles at 1 T as a function of the frequency for system #1.

4. Results discussion

The wide variety of results does not permit immediate careful analysis. For this reason, the comparison has been performed at 50 Hz for some magnetic and energetic properties. The BH curves at 50 Hz for every SMC system are reported in Fig. 26. System #2 shows deeper saturation and higher permeability, but it is important to remember that for the medium–high frequencies, the BH curves of system#2 decreased significantly (Fig. 17), whereas system#1 maintains stable B(H) characteristics (Fig. 14). The full hysteresis cycles at 1 T and 50 Hz are shown in Fig. 27. All systems show tight cycles at 50 Hz except system#3, which has poor magnetic properties. A unique favourable consideration for system#3 is that it is possible to advance in the investigation for high temperature withstanding varying the concentration of the dissolved reagent, modified process parameters (time, bath solution, etc.), or increment the number of layers. The highest electrical insulation has

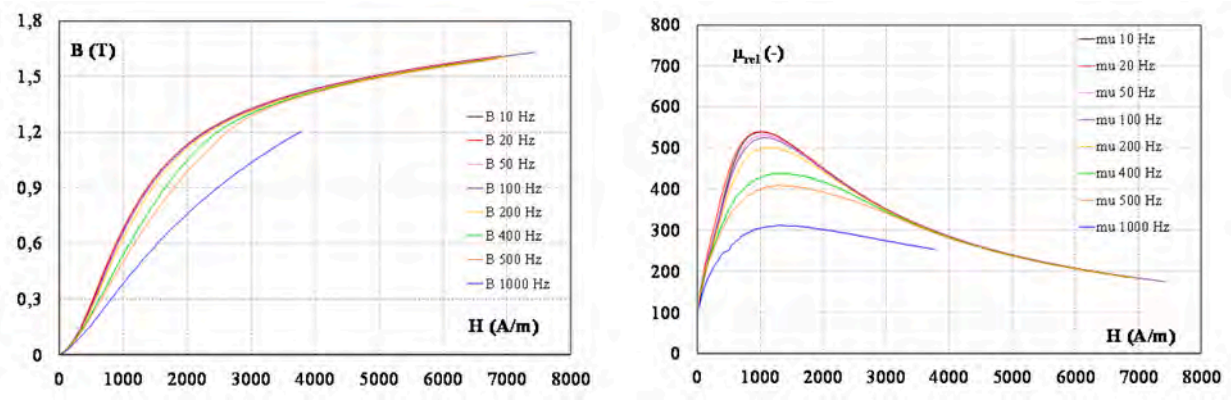


Fig. 17. BH curves and magnetic permeability as a function of the frequency for the system #2.

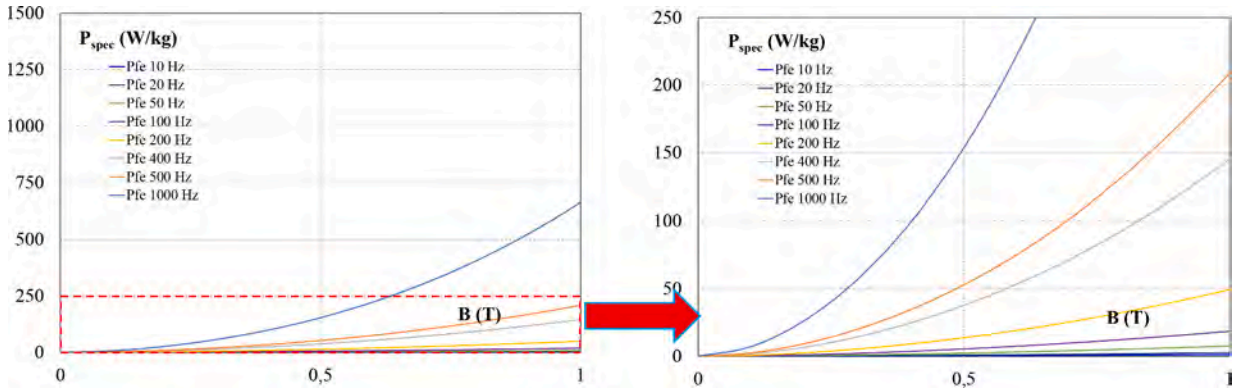


Fig. 18. Specific iron losses as a function of magnetic induction at different frequencies for system #2: full range and restricted to 250 W/kg.

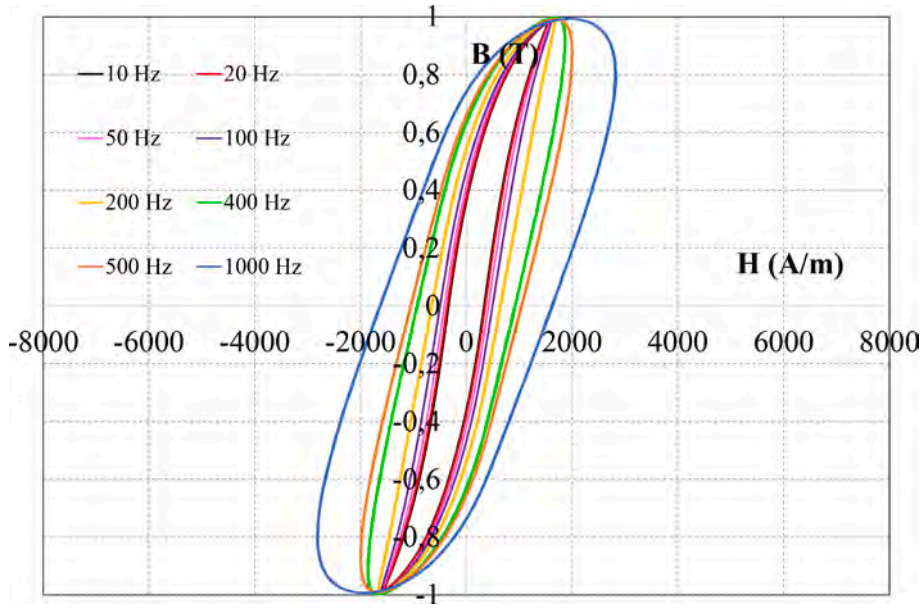


Fig. 19. Hysteresis cycles at 1 T as a function of the frequency for system #2.

system#1, mainly if taking into account all frequency ranges where system#2 becomes weaker, especially over 400 Hz, as shown in Fig. 19. The SMC produced with system#1 is acceptable for electrical machine applications.

Every proposed system represents a proposal of a specific research path, which gives emphasis to a particular property. Each path can be designed to lead to the optimization of the emerging properties, still reaching a compromise with the overall material performance. Since the hardest property to be obtained is a high temperatura withstanding, System #3 seems to be a good option to begin a future research path, even if the magnetic properties are not optimized at the moment.

Instead, the inductor properties are compared by measuring the

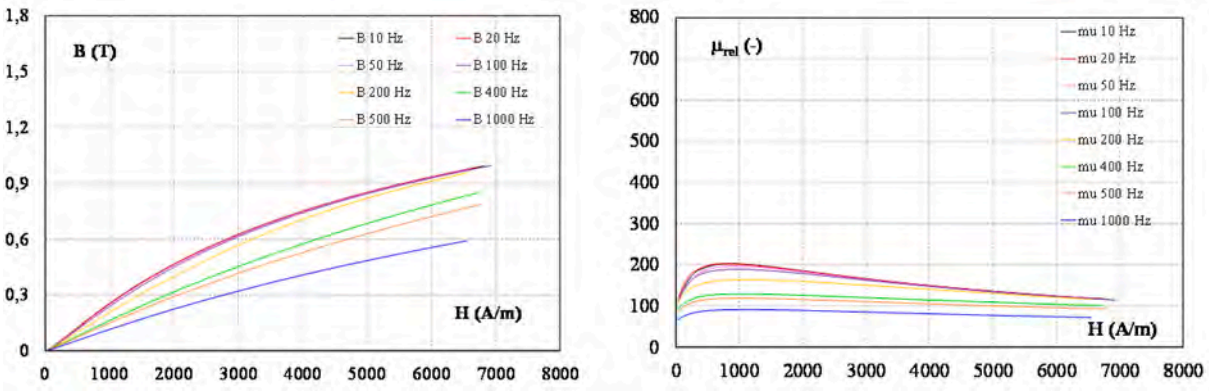


Fig. 20. BH curves and magnetic permeability as a function of the frequency for the system #3.

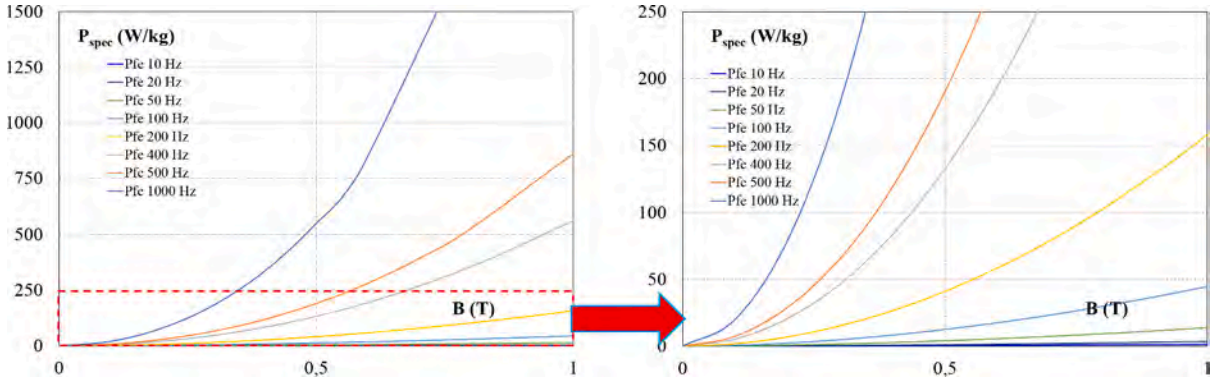


Fig. 21. Specific iron losses as a function of magnetic induction at different frequencies for system #3: full range and restricted to 250 W/kg.

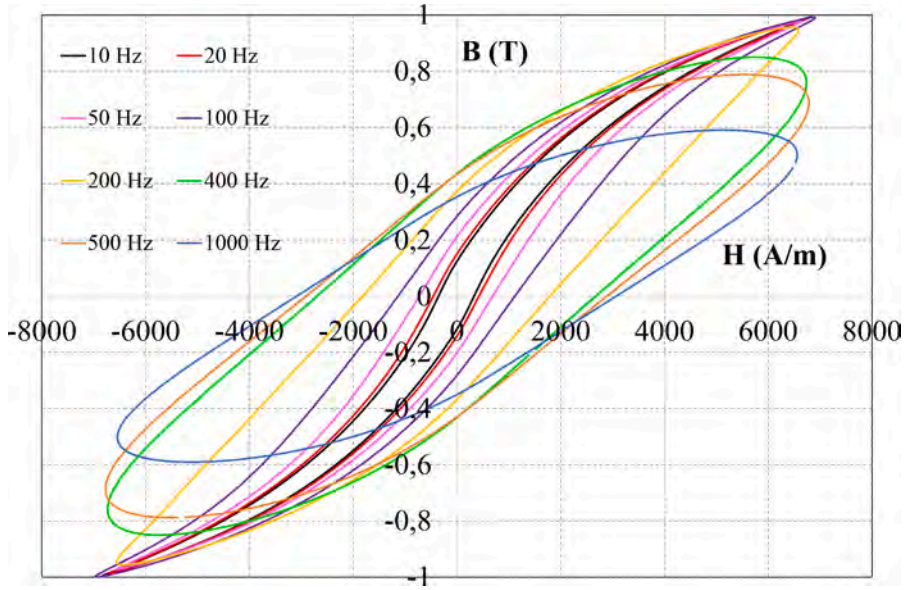


Fig. 22. Hysteresis cycles at 1 T as a function of the frequency for system #3.

inductance values using the RLC approach [53]. Each sample is wound with 75 coils with a 0.25 mm diameter enamelled copper wire. For this test, only system#1 and system#4 are used for their low eddy current losses in the wide frequency range. The inductance values until 1 MHz are reported in Fig. 28. The SMC with system#1 has a higher value than the one with system#4. On the other hand, the almost constant value for system#1 is just maintained until 20 kHz, while for system#4, the constant value range reaches 100 kHz. Owing to the higher frequency range, the SMC produced by coating system#4 is the most suitable for inductance applications.

Finally, the last comparison was conducted with the most common commercial SMC product, here named insulated iron powder compounds (I.I.P.C.). Such assessment has been carried out considering several parameters: magnetic, energetic and mechanical properties and

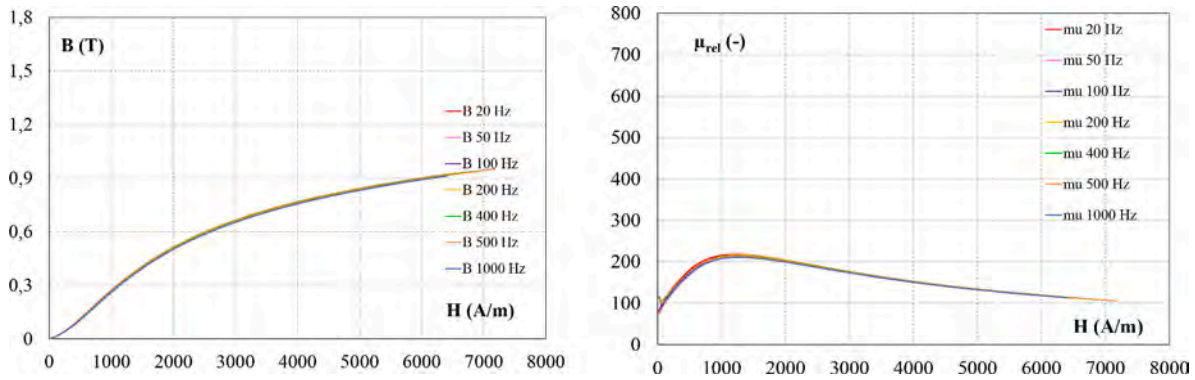


Fig. 23. BH curves and magnetic permeability as a function of the frequency for the system #4.

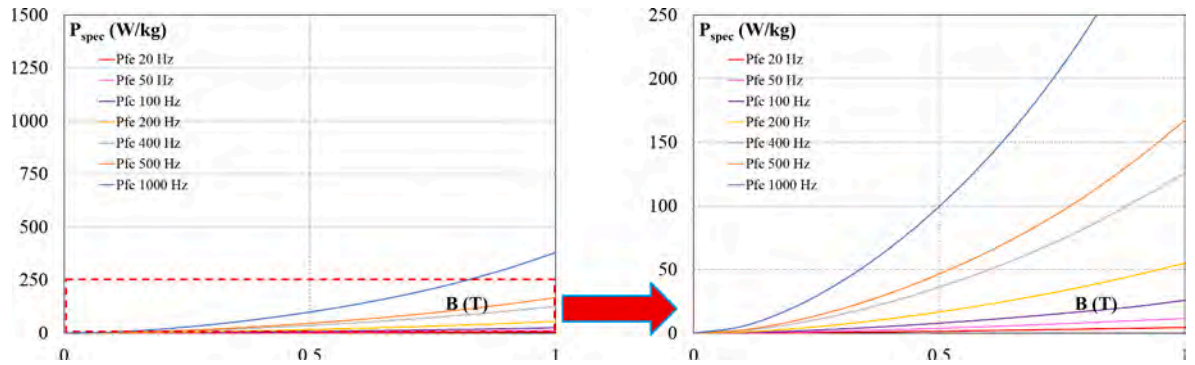


Fig. 24. Specific iron losses as a function of magnetic induction at different frequencies for system #4: full range and restricted to 250 W/kg.

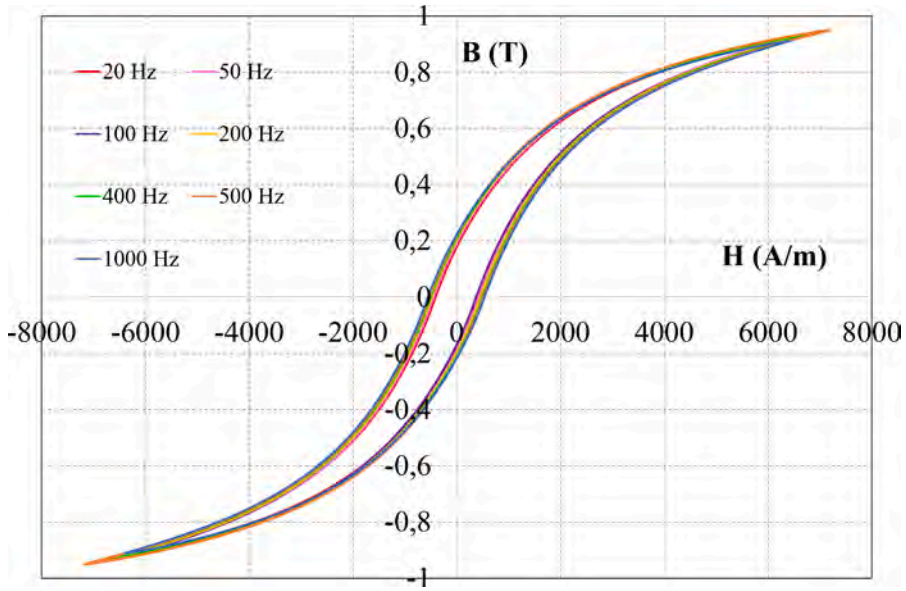


Fig. 25. Hysteresis cycles at 1 T as a function of the frequency for system #4.

Table 2
Transverse rupture strength results of proposed SMC materials.

Mechanical Strength TRS (MPa)	
System #1	110
System #2	191
System #3	87
System #4	31

heat treatment temperature (see Table 3). The I.I.P.C. SMCs are pressed at 800 MPa in the same shape as the analyzed samples. The heat treatment was done in the air at 550 °C but also could be applied in steam to improve mechanical properties. System #1 and #2 have similar magnetic permeability to I.I.P.C., but the BH curves show a higher saturation level than the commercial reference product. On the other hand, the I.I.P.C. shows the lowest iron losses @50 Hz and 1 T. The higher heat treatment temperature justifies such a result with respect to System#1 and #2, due to the hysteresis losses reduction. System#3 was treated at a

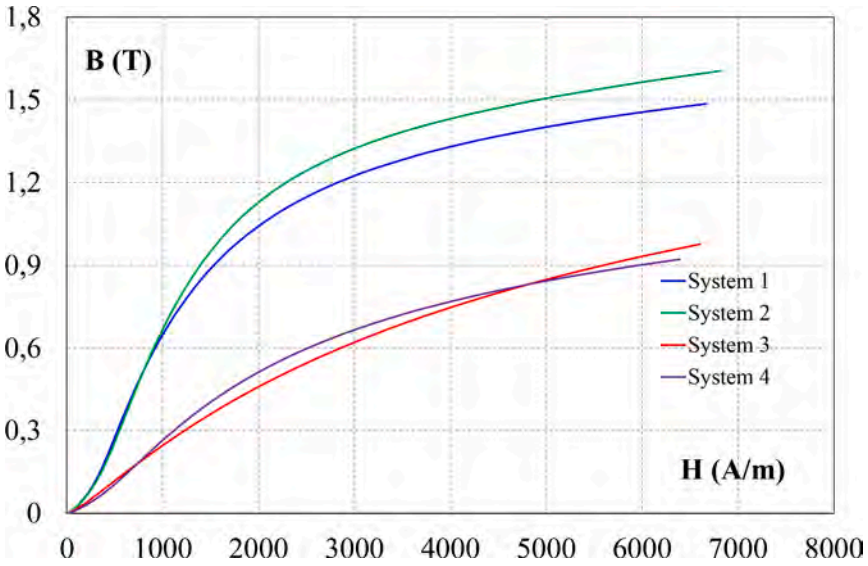


Fig. 26. BH curves at 50 Hz for all proposed SMC systems.

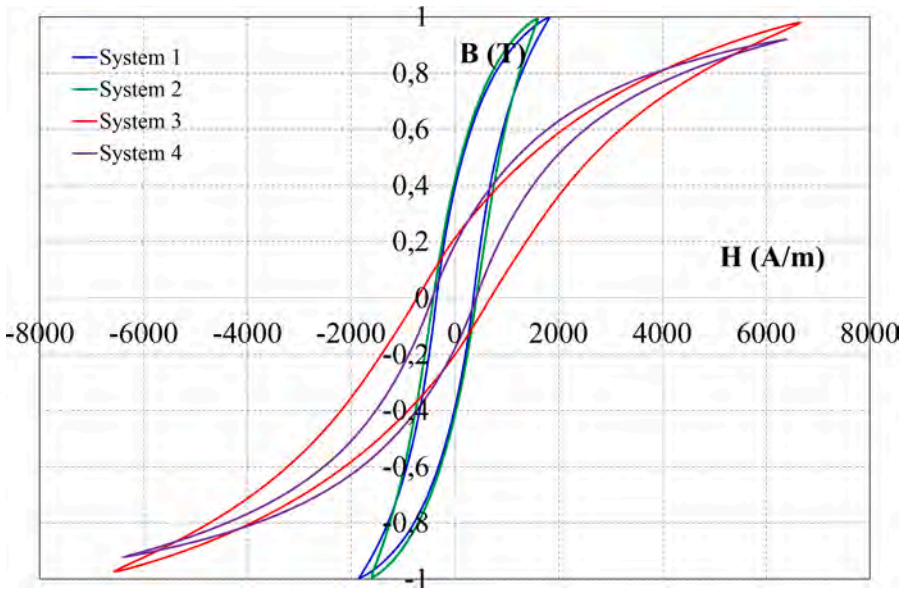


Fig. 27. Full hysteresis cycles at 1 T and 50 Hz for all proposed SMC systems.

higher temperature compared to the commercial product, but magnetic and energetic properties were insufficient. The I.I.P.C. has mechanical properties similar to System#1 but about half compared to System#2. Generally, the mentioned commercial product is not often used for inductance applications. However, a detailed optimization of the layers through the proposed technique can lead to an effective improvement of all properties, eventually with better results than SMC available on the market.

5. Conclusions

A novel insulating and binding layer-by-layer deposition process was presented with many solutions for SMC materials. The SMC coating produced by LbL techniques could have multifunctional behaviour, controlled number of layers, hybrid compositions, and nano dimensions. The demonstration of the potential of the proposed method is carried out with four different examples of produced SMC materials. Each of them represents a partial solution to a specific SMC problem: the energetic behaviour, the mechanical properties, the withstanding of the heat treatments and the application sectors. Some promising results have been obtained concerning the eddy current losses reduction and improved mechanical strength. Also, some solutions are suitable for a detailed study of electrical machine and inductor applications.

Future research work in this field is wide and can be applied to various devices, which is necessary to focus on particular material properties.

CRediT authorship contribution statement

Emir Pošković: Writing – review & editing, Writing – original draft, Validation, Methodology, Investigation, Formal analysis, Data curation, Conceptualization. **Fausto Franchini:** Validation, Software, Methodology, Investigation, Data curation, Conceptualization. **Marco Actis Grande:** Validation, Supervision, Resources, Methodology, Investigation. **Luca Ferraris:** Visualization, Validation, Supervision, Resources, Methodology, Data curation. **Federico Carosio:** Visualization,

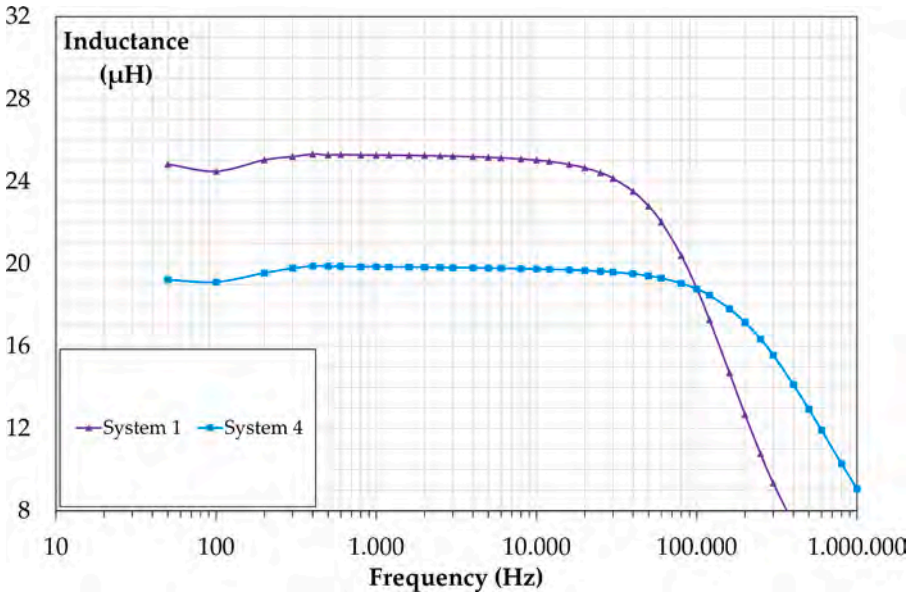


Fig. 28. Inductance value until 1 MHz for system#1 and system#4.

Table 3
Comparison between typical commercial product and proposed SMCs.

Proposed Coating Systems	Magnetic permeability	Magnetic induction @5000 A/m (T)	Iron losses @50 Hz and 1 T (W/kg)	Heat treatment temperature (°C)	Mechanical Strength TRS (MPa)
I.I.P.C.	486	1.30	5.47	550	100
System#1	522	1.40	6.52	180	110
System#2	539	1.51	7.57	500	191
System#3	200	0.85	13.87	750	87
System#4	218	0.84	11.48	300	31

Validation, Supervision, Resources, Methodology, Investigation, Conceptualization. **Alberto Tenconi:** Validation, Supervision, Resources, Methodology.

Declaration of competing interest

The authors declare that they have no known competing financial interests or personal relationships that could have appeared to influence the work reported in this paper.

Data availability

The data that has been used is confidential.

Acknowledgements

The part of research activities developed by Emir Pošković was carried out within the Ministerial Decree no. 1062/2021 and received funding from the FSE REACT-EU - PON Ricerca e Innovazione 2014-2020. This manuscript reflects only the authors' views and opinions, neither the European Union nor the European Commission can be considered responsible for them.

References

[1] A. Lepoutre et al., "Calculation of the GHG emissions of a European research project on electrified vehicles," *IEEE VPPC Conf.*, Gijon (Spain) 25-28 Oct. 2021, Conf. Proc. pp. 1-5, doi: 10.1109/VPPC53923.2021.9699266.
[2] P. Ramesh, N.C. Lenin, High power density electrical machines for electric vehicles—comprehensive review based on material technology, IEEE Trans. on Magn. 55 (11) (2019) 1–21, https://doi.org/10.1109/TMAG.2019.2929145.
[3] S. Karamanou et al., "A novel approach for plastic bonded magnets of the type MQU-F melt spun NdFeGaB-type alloys," *IEEE INTERMAG* Conf., Dublin (Ireland), 24-28 April 2017, Conf. Proc. pp. 1-1, doi: 10.1109/INTMAG.2017.8007670.
[4] E. Pošković, L. Ferraris, F. Carosio, F. Franchini, N. Bianchi, "Overview on bonded magnets realization, characterization and adoption in prototypes," *IEEE IECON Conf.*, Lisbon (Portugal), 14÷17 October 2019, pp. 1249-1254, doi: 10.1109/IECON.2019.8927827.
[5] S. Kontos, A. Ibrayeva, J. Leijon, G. Mörée, A.E. Frost, L. Schönström, K. Gunnarsson, P. Svedlindh, M. Leijon, S. Eriksson, An overview of MnAl permanent magnets with a study on their potential in electrical machines, MDPI Energies 13 (2020), https://doi.org/10.3390/en13215549.
[6] E. Pošković, F. Franchini, M. Ceroni, C. Innocenti, L. Ferraris, C. Sangregorio, A. Caneschi, M. Actis Grande, Study of an impact mill-based mechanical method for NdFeB magnet recycling, Metals 13 (6) (2020) 1103, https://doi.org/10.3390/met13061103.
[7] A. Krings, A. Boglietti, A. Cavagnino, S. Sprague, Soft magnetic material status and trends in electric machines, IEEE Trans. Ind. Electron. 64 (3) (2017) 2405–2414, https://doi.org/10.1109/TIE.2016.2613844.
[8] J.M. Silveyra, E. Ferrara, D.L. Huber, T.C. Monson, Soft magnetic materials for a sustainable and electrified world, AAAS Science 362 (2018), https://doi.org/10.1126/science.aao0195.
[9] E. Pošković, F. Franchini, L. Ferraris, E. Fracchia, J. Bidulska, F. Carosio, R. Bidulsky, M. Actis Grande, Recent advances in multi-functional coatings for soft magnetic composites, MDPI Materials 14 (22) (2021), https://doi.org/10.3390/ma14226844.
[10] E.A. Périgo, B. Weidenfeller, P. Kollár, J. Füzer, Past, present and future of soft magnetic composites, Appl. Phys. Rev. 5 (3) (2018) 031301, https://doi.org/10.1063/1.5027045.
[11] A. Schoppa, P. Delarbre, A. Schatz, Optimal use of soft magnetic powder composites (SMC) in electrical machines, Mater. Sci. (2013).
[12] M. Kącki, M.S. Rylko, J.G. Hayes, C.R. Sullivan, "Magnetic material selection for EMI filters", *IEEE ECCE Conf.*, Cincinnati (USA), 1÷5 October 2017; Conf. Proc. pp. 2350–2356, doi: 10.1109/ECCE.2017.8096456.
[13] J. He, H. Yuan, M. Nie, H. Guo, H. Yu, Z. Liu, R. Sun, Soft magnetic materials for power inductors: state of art and future development, ISSN 2772-9494, Mater. Today Electronics 6 (2023) 100066, https://doi.org/10.1016/j.mtelec.2023.100066.
[14] V. Chaudhary, S.A. Mantri, R.V. Ramanujan, R. Banerjee, Additive manufacturing of magnetic materials, ISSN 0079-6425, Prog. Mater Sci. 114 (2020) 100066, https://doi.org/10.1016/j.pmatsci.2020.100688.
[15] F. Bernier, M. Ibrahim, M. Mihai, Y. Thomas, J.-M. Lamarre, Additive manufacturing of soft and hard magnetic materials used in electrical machines, Met. Powder Rep. 75 (6) (2020) 334–343, https://doi.org/10.1016/j.mprp.2019.12.002.
[16] T.N. Lamichhane, L. Sethuraman, A. Dalagan, H. Wang, J. Keller, M. P. Paranthaman, Additive manufacturing of soft magnets for electrical

machines—a review, ISSN 2542-5293, Materials Today Physics 15 (2020) 100255, https://doi.org/10.1016/j.mtphys.2020.100255.
[17] E.A. Périgo, J. Jacimovic, F. García Ferré, L.M. Scherf, Additive manufacturing of magnetic materials, ISSN 2214-8604, Addit. Manuf. 30 (2019) 100870, https://doi.org/10.1016/j.addma.2019.100870.
[18] M. Quercio, et al., Functional characterization of L-PBF produced FeSi2.9 soft magnetic material, in: 2022 International Conference on Electrical Machines (ICEM), 2022, pp. 531–537, https://doi.org/10.1109/ICEM51905.2022.9910684.
[19] A. Schoppa, P. Delarbre, Soft magnetic powder composites and potential applications in modern electric machines and devices, IEEE Trans. Magn. 50 (4) (2014) 1613–1616, https://doi.org/10.1109/TMAG.2013.2290135.
[20] M.M. Dias, H.J. Mozetic, J.S. Barboza, R.M. Martins, L. Pelegrini, L. Schaeffer, Influence of resin type and content on electrical and magnetic properties of soft magnetic composites (SMCs), Powder Technol. 237 (2013) 213–220, https://doi.org/10.1016/j.powtec.2013.01.006.
[21] H. Shokrollahi, K. Janghorban, Soft magnetic composite materials (SMCs), J. Mater. Process. Technol. 189 (2007) 1–12, https://doi.org/10.1016/j.jmatprotec.2007.02.034.
[22] C. Xia, Y. Peng, Y. Yi, H. Deng, Y. Zhu, G. Hu, The magnetic properties and microstructure of phosphated amorphous FeSiCr/silane soft magnetic composite, J. Magn. Magn. Mater. 474 (2019) 424–433, https://doi.org/10.1016/j.jmmm.2018.11.058.
[23] S. Lee, M. Choi, J. Kim, Magnetic properties of pure iron soft magnetic composites coated by manganese phosphates, IEEE Trans. Magn. 53 (2017) 1–4, https://doi.org/10.1109/TMAG.2017.2718113.
[24] H.-I. Hsiang, L.-F. Fan, J.-J. Hung, Phosphoric acid addition effect on the microstructure and magnetic properties of iron-based soft magnetic composites, J. Magn. Magn. Mater. 447 (2018) 1–8, https://doi.org/10.1016/j.jmmm.2017.08.096.
[25] A.H. Taghvaei, H. Shokrollahi, K. Janghorban, Properties of iron-based soft magnetic composite with iron phosphate–silane insulation coating, J. Alloys Compd. 481 (2009) 681–686, https://doi.org/10.1016/j.jallcom.2009.03.074.
[26] M. Strečková, J. Füzer, L. Kobera, J. Brus, M. Fáberová, R. Bureš, P. Kollár, M. Lauda, Ľ. Medvecký, V. Girman, H. Hadraba, M. Bat'ková, I. Bat'ko, A comprehensive study of soft magnetic materials based on FeSi spheres and polymeric resin modified by silica nanorods, Mater. Chem. Phys. 147 (3) (2014) 649–660, https://doi.org/10.1016/j.matchemphys.2014.06.004.
[27] W. Ding, L. Jiang, Y. Liao, J. Song, B. Li, G. Wu, Effect of iron particle size and volume fraction on the magnetic properties of Fe/silicate glass soft magnetic composites, J. Magn. Magn. Mater. 378 (2015) 232–238, https://doi.org/10.1016/j.jmmm.2014.09.019.
[28] X.A. Fan, Z.Y. Wu, G.Q. Li, J. Wang, Z.D. Xiang, Z.H. Gan, High resistivity and low core loss of intergranular insulated Fe–6.5 wt.% Si/SiO2 composite compacts, Mater. Des. 89 (2016) 1251–1258, https://doi.org/10.1016/j.matdes.2015.10.087.
[29] Z.Y. Wu, Z. Jiang, X.A. Fan, L.J. Zhou, W.L. Wang, K. Xu, Facile synthesis of fe-6.5wt%Si/SiO2 soft magnetic composites as an efficient soft magnetic composite material at medium and high frequencies, J. Alloys Compd. 742 (2018) 90–98, https://doi.org/10.1016/j.jallcom.2018.01.307.
[30] L. Liu, Q. Yue, G.Q. Li, K. Xu, J. Wang, Z.Y. Wu, X.A. Fan, Influence of SiO2 insulation layers thickness distribution on magnetic behaviors of fe-Si@SiO2 soft magnetic composites, J. Phys. Chem. Solids 132 (2019) 76–82, https://doi.org/10.1016/j.jpcs.2019.04.016.
[31] B. Meng, B. Yang, X. Zhang, B. Zhou, X. Li, R. Yu, Combinatorial surface coating and greatly-improved soft magnetic performance of Fe/Fe3O4/resin composites, Mater. Chem. Phys. 242 (2020) 122478, https://doi.org/10.1016/j.matchemphys.2019.122478.
[32] J. Li, J. Yu, W. Li, S. Che, J. Zheng, L. Qiao, Y. Ying, The preparation and magnetic performance of the iron-based soft magnetic composites with the Fe@Fe3O4 powder of in situ surface oxidation, J. Magn. Magn. Mater. 454 (2018) 103–109, https://doi.org/10.1016/j.jmmm.2018.01.061.
[33] Z. Luo, X.A. Fan, W. Hu, F. Luo, J. Wang, Z. Wu, X. Liu, G. Li, Y. Li, Formation mechanism and enhanced magnetic properties of Fe–Si/Fe2SiO4 soft magnetic composites transformed from fe-6.5 wt%Si/α-Fe2O3 core-shell composites, J. Alloys Compd. 817 (2020) 152803, https://doi.org/10.1016/j.jallcom.2019.152803.
[34] Z. Luo, X.A. Fan, W. Hu, F. Luo, J. Wang, Z. Wu, X. Liu, G. Li, Y. Li, High performance fe-si soft magnetic composites coated with novel insulating-magnetic-insulating (IMI) layer, J. Magn. Magn. Mater. 496 (2020) 165937, https://doi.org/10.1016/j.jmmm.2019.165937.
[35] L. Yan, B. Yan, Microstructure and magnetic properties of Fe–6.5 wt.%Si/MnZn (Fe2O4)2 composites with core-shell structure prepared by spark plasma sintering, Int. J. Mod. Phys. B 31 (2017) 1744013, https://doi.org/10.1142/S0217979217440131.
[36] M. Wang, Z. Zan, N. Deng, Z. Zhao, Preparation of pure iron/Ni–Zn ferrite high strength soft magnetic composite by spark plasma sintering, J. Magn. Magn. Mater. 361 (2014) 166–169, https://doi.org/10.1016/j.jmmm.2014.02.055.
[37] E. Pošković, F. Franchini, F. Carosio, M. Actis Grande, L. Ferraris, "Application of impact mill technique for the production of soft magnetic composite materials," *In Proceedings of the AIM 2020*, Naples, Italy, 20 January 2021.
[38] E. Pošković, F. Carosio, L. Ferraris, F. Franchini, M. Actis Grande, "Processo per la produzione di materiali magnetici nanorivestiti" Italy National Patent No. 102021000026681, October 18, 2021.
[39] E. Pošković, F. Carosio, L. Ferraris, F. Franchini, M. Actis Grande, " PROCESS FOR THE PRODUCTION OF NANO-COATED FERROMAGNETIC MATERIALS" PCT Patent No. WO2023067471, April 27, 2023.
[40] M. Marcioni, M. Zhao, L. Maddalena, T. Pettersson, R. Avolio, R. Castaldo, L. Wågberg, F. Carosio, Layer-by-layer-coated cellulose fibers enable the production of porous, flame-Retardant, and lightweight materials, ACS Appl. Mater. Interfaces 15 (30) (2023) 36811–36821, https://doi.org/10.1021/acsami.3c06652.
[41] D. Battegazzore, A. Frache, F. Carosio, "Layer-by-Layer nanostructured interphase produces mechanically strong and flame retardant bio-composites," *Composites Part B: Engineering*, **200**, 2020, 108310, ISSN 1359-8368, https://doi.org/10.1016/j.compositesb.2020.108310.
[42] L. Maddalena, F. Carosio, J. Gomez, G. Saracco, A. Fina, Layer-by-layer assembly of efficient flame retardant coatings based on high aspect ratio graphene oxide and chitosan capable of preventing ignition of PU foam, Polym. Degrad. Stab. 152 (2018) 1–9, https://doi.org/10.1016/j.polymdegradstab.2018.03.013.
[43] T. Jiang, L. Maddalena, J. Gomez, F. Carosio, A. Fina, Polyelectrolytes enabled reduced graphite oxide water dispersions: effects of the structure, Molecular weight, and Charge density, Polymers 14 (19) (2022) 4165, https://doi.org/10.3390/polym14194165.
[44] N. Mazur, S. Salviati, H. Huinink, A. Fina, F. Carosio, H. Fischer, O. Adan, Impact of polymeric stabilisers on the reaction kinetics of SrBr 2, ISSN 0927-0248, Sol. Energy Mater. Sol. Cells 238 (2022) 111648, https://doi.org/10.1016/j.solmat.2022.111648.
[45] W. Tabaka, S. Timme, T. Lauterbach, L. Medina, L.A. Berglund, F. Carosio, S. Duquesne, B. Schartel, Bench-scale fire stability testing – assessment of protective systems on carbon fibre reinforced polymer composites, ISSN 0142-9418, Polym. Test. 102 (2021) 107340, https://doi.org/10.1016/j.polymertesting.2021.107340.
[46] P. Samanta, A. Samanta, C. Montanari, Y. Li, L. Maddalena, F. Carosio, L. A. Berglund, Fire-retardant and transparent wood biocomposite based on commercial thermoset, ISSN 1359-835X, Compos. A Appl. Sci. Manuf. 156 (2022) 106863, https://doi.org/10.1016/j.compositesa.2022.106863.
[47] E. Guido, J. Alongi, C. Colleoni, A. Di Blasio, F. Carosio, M. Verelst, G. Malucelli, G. Rosace, Thermal stability and flame retardancy of polyester fabrics sol–gel treated in the presence of boehmite nanoparticles, P*Olymer Degradation and Stability* 98 (9) (2013) 1609–1616, https://doi.org/10.1016/j.polymdegradstab.2013.06.021.
[48] S. Tumanski., "Magnetic Materials from: Handbook of Magnetic Measurements", *CRC Press*, 23 June 2011, https://doi.org/10.1201/b10979.
[49] E. Pošković, F. Franchini, L. Ferraris, F. Carosio, M. Actis Grande, Rapid Characterization method for SMC materials for a Preliminary selection, MDPI. Appl. Sci. 11 (24) (2021), https://doi.org/10.3390/app112412133.
[50] C. Appino, E. Ferrara, F. Fiorillo, L. Rocchino, C. Ragusa, J. Sievert, T. Belgrand, C. Wang, P. Denke, S. Siebert, Y. Norgren, K. Gramm, S. Norman, R. Lyke, M. Albrecht, X. Zhou, W. Fan, X. Guo, M. Hall, C. Appino, C. Beatrice, F. Fiorillo, C. Ragusa, International comparison on SST and epstein measurements in grain-oriented fe-si sheet steel, Int. J. Appl. Electromagn. Mech. 48 (2,3) (2015) 123–133, https://doi.org/10.3233/JAE-151978.
[51] Z. Gmyrek, Single sheet tester with Variable dimensions, IEEE Trans. Instrum. Meas. 65 (7) (July 2016) 1661–1668, https://doi.org/10.1109/TIM.2016.2540839.
[52] E. Pošković, L. Ferraris, F. Franchini, R. Bidulsky, M. Actis Grande, "Novel SMC Materials with the Insulating Layer Treated at High Temperature", *EPMA EURO PM2019*, Maastricht (Netherlands), 13÷16 October 2019, Conf. Proc..
[53] E. Pošković, F. Franchini, and L. Ferraris, "Effect of the Insulating Layer on the Properties of SMC Inductors," *Applied Sciences*, **12**, no. 17, p. 8756, Aug. 2022, doi: 10.3390/app12178756.